Chinese Chemical Letters 34 (2023) 107671

Contents lists available at ScienceDirect

Chinese Chemical Letters

journal homepage: www.elsevier.com/locate/cclet

Discovery of novel triple targeting G–quadruplex and topoisomerase 1/2 ligands from natural products evodiamine and rutaecarpine

Haibo Wang[a,b,1], Xuexin Bai[b,1], Yahui Huang[b], Yueru Chen[c], Guoqiang Dong[b], Tianmiao Ou[c], Shanchao Wu[b,*], Defeng Xu[a,*], Chunquan Sheng[b,*]

[a] National & Local Joint Engineering Research Center for High-efficiency Refining and High-quality Utilization of Biomass, School of Pharmacy, Changzhou University, Changzhou 213164, China
[b] Department of Medicinal Chemistry, School of Pharmacy, Second Military Medical University, Shanghai 200433, China
[c] School of Pharmaceutical Sciences, Sun Yat-sen University, Guangzhou 510006, China

ARTICLE INFO

Article history:
Received 4 April 2022
Revised 7 July 2022
Accepted 8 July 2022
Available online 9 July 2022

Keywords:
Indolopyridoquinazoline
G–quadruplex
Topoisomerase
Structure-activity relationship
Antitumor activity

ABSTRACT

Inspired by the indolopyridoquinazoline scaffold of natural products evodiamine and rutaecarpine, novel triple G4 and Top1/2 ligands were rationally designed and synthesized. Systematic structure–activity relationship (SAR) studies led to the discovery of compound **15g**, which effectively induced and stabilized G4 and inhibited Top1/2 with potent antitumor activity. Compound **15g** represents a valuable chemical tool or lead compound for antitumor drug discovery. This proof-of-concept study also validated the feasibility of using planar natural products scaffold as templates to design new G4 ligands.

Topoisomerases (Top), an important component of nuclear enzymes, play an essential role in modulating DNA supercoiling during DNA transcription, replication, and chromatin assembly [1]. DNA topoisomerases Top1 and Top2 induce transient DNA single-strand or double-strand breaks by cleaving single or double DNA strands, respectively [1]. In the past decades, important progress has been achieved in the development of Top inhibitors [2–5]. Several Top inhibitors, such as topotecan (TPT, a Top1 inhibitor) and etoposide (Eto, a Top2 inhibitor), have been approved and successfully applied in clinic for cancer therapy [6].

In the field of DNA targeted drugs, small molecules that stabilize G-quadruplex (G4) DNA are also considered as promising anticancer strategy [7–11]. G4 structures are formed by stacking of two or more G-quartets, *i.e.*, cyclic planar arrangements of four guanines [12–14]. When promoters are folded into G4 structures, transcription is repressed at oncogene level [15]. Since oncogenes are overexpressed only in cancer cells [16], antitumor drugs that simultaneously promoting G-quadruplex formation also at oncogene promoters level could dramatically reinforce the anticancer activity [17]. Thus, simultaneously targeting G4 and Top would be a promising strategy in antitumor drug discovery. Moreover, synergistic antitumor effects between G4 and Top ligands, such as dibenzoquinoxaline (**1**) [18], indenoisoquinoline (**2**) [19] and quinolinoquinoxaline (**3**) [20] have been confirmed (Fig. 1A).

G4 ligands generally bear a large planar heteroaromatic core and a side chain with a terminal amine group [20–23]. For example, G4 ligands BRACO-19 (**4**) [17–19], Pidnarulex (CX-5461, **5**) [24] and quindoline (**6**) (Fig. 1A) [7,25] have been reported to possess potent antitumor potency [26]. Natural products containing planar polycyclic system offer favorable templates to design new G4 ligands by conjugating alkyl amine side chains [20].

Evodiamine (**7a**) and rutaecarpine (**8a**) (Fig. 1B) are two main bioactive indolopyridoquinazoline alkaloids isolated from Evodia rutaecarpa, and have diverse biological activities [27–29]. Several evodiamine derivatives (*e.g.*, compounds **7b**, **7c** and **7d**, Fig. 1B) were identified as Top1/2 dual inhibitors with potent antitumor activities by our group [30–32]. The indolopyridoquinazoline skeleton bearing a large planar heteroaromatic core shares structural similarity with reported G4 ligands (Fig. 1C). Thus, we envisioned that G4 and Top1/2 ligands could be designed by incorporating the alkyl amine-containing moiety into the indolopyridoquinazoline scaffold. As a conceptual validation study, herein the first G4 and Top1/2 triple ligands were designed and assayed (Fig. 1D).

The synthetic route of evodiamine derivatives were depicted in Scheme 1 and Table S1 (Supporting information). In the presence

* Corresponding authors.
E-mail addresses: wushanchao07_2@126.com (S. Wu), markxu@cczu.edu.cn (D. Xu), shengcq@smmu.edu.cn (C. Sheng).
[1] These authors contributed equally to this work.

https://doi.org/10.1016/j.cclet.2022.07.014
1001-8417/

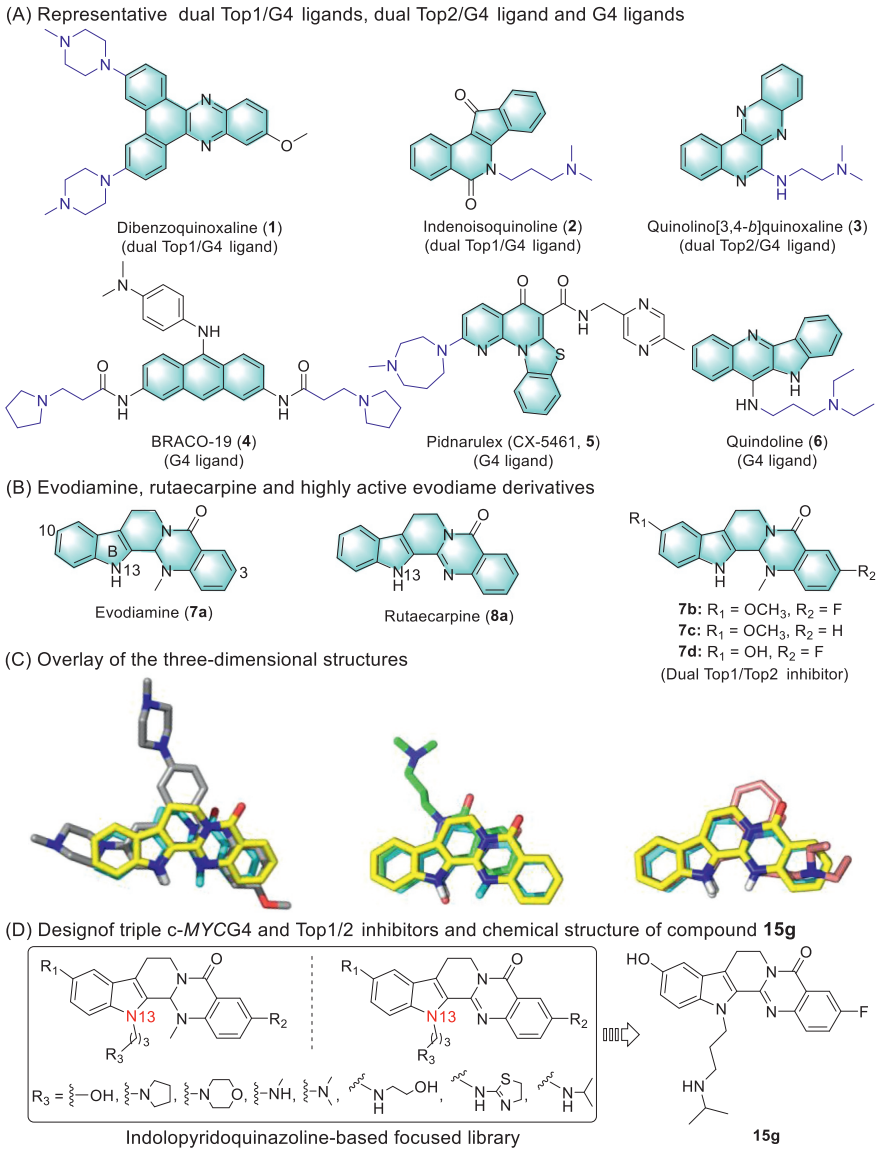

Fig. 1. Chemical structures of representative G4 and Top1/2 ligands and design rationale of target compounds. (A) Representative G4 ligands, dual Top1/G4 ligands and dual Top2/G4 ligand. The scaffold and side chain are depicted in different colors. (B) Chemical structures of evodiamine, rutaecarpine and highly active evodiamine derivates. (C) Overlay of the three-dimensional structures of evodiamine (carbon in yellow), rutaecarpine (carbon in blue) and reported G4 ligands (**1**, carbon in gray; **2**, carbon in green; and **3**, carbon in pink) in their energy minimized states. (D) Design of triple G4 and Top1/2 ligands and chemical structure of compound **15g**.

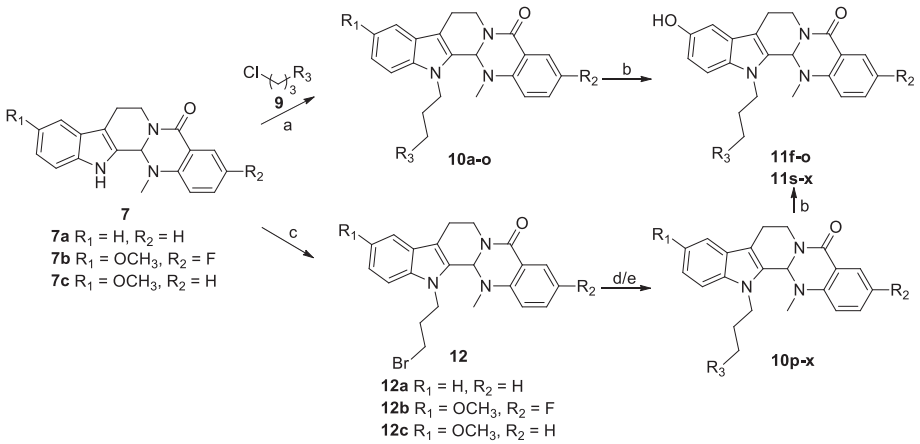

Scheme 1. Synthesis of evodiamine derivatives. Reagents and conditions: (a) DMF, NaH, 65 °C, 12 h, yield 43%–78%; (b) DCM, BBr_3, under N_2, −78 °C, 2 h, yield 24%–85%; (c) DMF, KOH, 1,3-dibromopropane, r.t., 12 h, yield 35%–80%; (d) **10p-q**, **10s-t**, **10v-w**: DMF, K_2CO_3, 65 °C, 12 h, yield 32%–60%; (e) **10r**, **10u**, **10x**: MeCN, r.t., 72 h, yield 44%–81%.

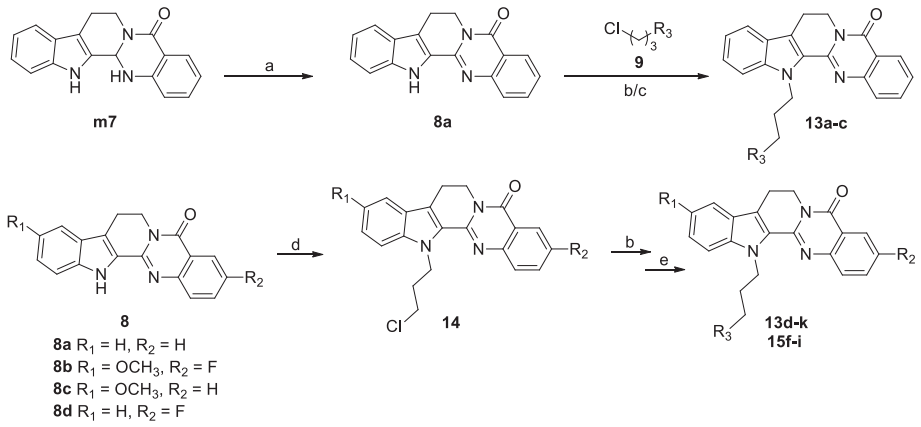

Scheme 2. Synthesis of rutaecarpine derivatives. Reagents and conditions: (a) DCM, DDQ, r.t., 8 h, yield 45%–55%; (b) **13a**, **13b**, **13d-k**: DMF, Cs_2CO_3, 65 °C, 12 h, yield 21%–25%; (c) **13c**: DMF, NaH, 65 °C, 12 h, yield 8%; (d) DMF, KOH, 1–bromo-3–chloropropane, r.t., 12 h, yield 19%–22%; (e) **15f-i**: DCM, BBr_3, under N_2, −78 °C, 2 h, yield 44%–98%.

of sodium hydride (NaH), target compounds **10a-o** were obtained by nucleophilic substitution reaction *via* treating compounds **7** [27] with various commercially available 3–chloro propyl amines (**9**). Target compounds **11f-o** were obtained by demethylation of **10f-o** in the presence of BBr_3 at −78 °C. Similarly, intermediate **12** was prepared from compounds **7** with 1,3-dibromopropane reaction in the presence of potassium hydroxide (KOH). Then, **12** was treated various commercially available 3–chloro propyl amines (**9**) to afford target compounds **10p-x**. Compounds **11s-x** were obtained by demethylation of **10s-x** in the presence of BBr_3 at −78 °C.

A similar strategy was applied for the synthesis of rutaecarpine derivatives **13a-c**, **13d-k** and **15f-i** (Scheme 2). Intermediate **m7** was prepared according to the reported procedure [31]. Intermediate **m7** was reacted with 2,3-dichloro-5,6-dicyano-1,4-benzoquinone (DDQ) *via* oxidation reaction to give rutaecarpine (**8a**). Then, target compounds **13a-c** were prepared by nucleophilic substitution reaction *via* treating intermediates **8a** with various commercially available 3–chloropropyl amines (**9**). Similarly, intermediate **14** was prepared by the treatment of intermediates **8** with 1–bromo-3-chloropropane reaction in the presence of potassium hydroxide (KOH). Compounds **13d-k** and **15f-i** were obtained by a similar protocol described in Scheme 1.

Initially, a total of 40 evodiamine analogues were designed and synthesized by incorporating various alkyl amine side chains onto the evodiamine *N*13 position (Scheme 1, Table S1). We first evaluated the evodiamine derivatives affinities to a typic c-*MYC*G4 by the fluorescence resonance energy transfer (FRET) quenching and FRET melting assays [18,19]. Since c-*MYC* is one of the most important oncogenes that is overexpressed in more than 80% of cancer cells and contributes to cell proliferation, angiogenesis, metastasis and apoptosis [8,33]. Moreover, nuclease hypersensitive element (NHE III_1) controls 85%–90% of c-*MYC* transcriptional activity, which folds into a DNA G-quadruplex (G4) under the transcription-associated negative supercoiling and thus silences c-*MYC* transcription [9,33,34]. The results showed that template molecules **7d** and **8a** were unable to induce and stabilize c-*MYC*G4 (Fig. 2A). After introducing the side chain, only compound **11v** decreased the relative fluorescence intensity by more than 42% at the concentration of 100 μmol/L (Fig. S1 in Supporting information). Moreover, only three compounds (**10g**, **10t** and **11g**) increased the T_m values of c-*MYC*G4 by more than 10 °C at the concentration of 10 μmol/L (Fig. S1). These results suggested that the scaffold of evodiamine was unfavorable to design potent c-*MYC*G4 ligands. In addition, terminal alkyl amine groups favorable for the activity (*e.g.,* thiazolyl, isopropyl, dimethyl and methyl substituents) were used in the next round of structural modification.

Then, the rutaecarpine scaffold was investigated and 15 *N*13-substituted derivatives were designed and assayed (Scheme 2, Table S2 in Supporting information). To our delight, 14 out of 15 target compounds exhibited potent c-*MYC*G4 binding and stabilizing activities at the concentration of 100 μmol/L and 10 μmol/L, respectively (relative decrease of fluorescence intensity: 56.7% to 96.6%; ΔT_m range: 13.3 °C to 32.0 °C (Figs. 2A and B, Table S3 in Supporting information). Nine compounds (**13f**, **13g**, **13h**, **13i**, **13j**, **13k**, **15g**, **15h** and **15i**) decreased the relative fluorescence intensity by more than 70% and increased the T_m value of c-*MYC*G4 by more than 20 °C (Table 1). Moreover, introducing hydroxyl or methoxyl group on the rutaecarpine scaffold led to enhanced c-*MYC*G4 binding and stabilizing activities (**15h** > **13j** > **13f** > **13d**, **13g** > **15g** > **13k** > **15i** > **13e**, Table 1). Notably, *N*13-substituents also played an important role in c-*MYC*G4 binding and stabilization (Fig. 2B, Table 1). For example, compounds with *N*13-(isopropylamino)propyl side chain exhibited better c-*MYC*G4 stabilizing activity than those with *N*13-(thiazolylamino)propyl group (**13e** > **13d**, **13g** > **13f**, **13i** > **13h**, **13k** > **13j**, **15g** > **15f**, **15i** > **15h**).

The compounds with more than 70% relative fluorescence intensity decrease were further selected to evaluate the Top inhibitory activities using the DNA cleavage assay [32]. As shown in Figs. 2C and D, 7 out of 13 compounds (**13e**, **13h**, **13i**, **13k**, **15g**, **15h** and **15i**) were active against Top1 at the concentration of 50 μmol/L and 25 μmol/L, respectively. The DNA bands treated with compounds **13e** and **13h** were broadened, which indicated that they had weak Top1 inhibitory activities. However, at a lower concentration of 1 μmol/L, two compounds (**15g** and **15i**) were still active (Fig. 2E). Moreover, 7 out of 13 compounds were active against Top2 at the concentration of 50 μmol/L (Fig. 2F). More specifically, compounds with *N*13-(isopropylamino)propyl or *N*13-(thiazolylamino)propyl side chain exhibited potent Top activities, which were consistent with their c-*MYC*G4 binding and stabilizing activities. Compounds **13i**, **15g**, **15h** and **15i** were validated as novel c-*MYC*G4/Top1/Top2 triple inhibitors.

On the basis of the c-*MYC*G4 and Top inhibitory activities, compound **15g** (Fig. 1D) was finally selected for further mechanism studies. Circular dichroism (CD) titration assay revealed that the signature of a parallel c-*MYC*G4 was maintained (Fig. 3A). Fluorescence-based binding assay indicated that compound **15g** showed strong c-*MYC*G4 binding activity with binding affinity K_d value of 156 nmol/L (Fig. 3B). ^{1}H nuclear magnetic resonance (^{1}H NMR) titration experiments were conducted to exam-

Table 1
The c-*MYC*G4 binding and stabilizing activities of *N*13-alkyl amine substituted rutaecarpine by fluorescence FRET quenching and FRET melting assays.[a]

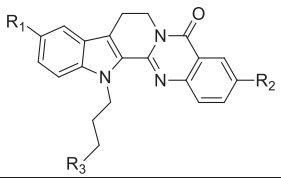

Compound	R_1	R_2	R_3	FRET-quenching (%)	FRET-melting ΔT_m (°C)
DMSO	-	-	-	100.00	-
KCl	-	-	-	60.03	-
Rutaecarpine (**8a**)	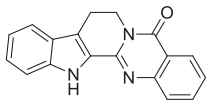		102.32		0.97
13a	H	H		43.30	13.30
13b	H	H		38.62	16.30
13c	H	H		21.42	15.30
13d	H	H	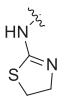	22.50	16.87
13e	H	H		26.79	17.97
13f	OCH_3	F		25.70	25.43
13g	OCH_3	F		3.39	23.86
13h	OCH_3	H		18.83	25.06
13i	OCH_3	H		13.14	27.40
13j	H	F		19.96	22.19
13k	H	F		6.45	22.22
15f	OH	F		96.60	18.22
15g	OH	F		7.05	32.02
15h	OH	H		13.35	20.97
15i	OH	H		20.55	24.93

[a] The values are the mean of at least two independent experiments.

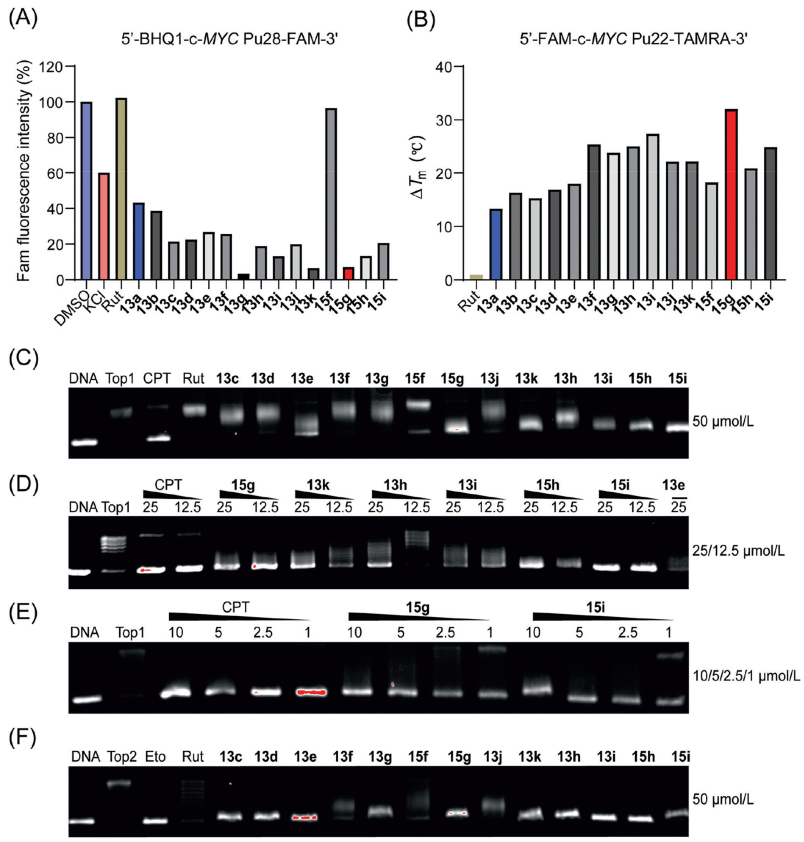

Fig. 2. c-*MYC*G4 binding and stabilizing activity and Top1/2 inhibitory activity of rutaecarpine derivatives. (A) FRET quenching assay of DMSO, 100 mmol/L K^+, rutaecarpine and its analogues in the presence of labeled c-*MYC*G4. KCl (100 mmol/L) was employed as positive control in FRET-quenching assay, which decreased the relative fluorescence intensity by 42%. (B) Thermal stabilization values (ΔT_m) of c-*MYC*G4 in the presence of rutaecarpine and its analogues by FRET melting assays. FRET-melting assay was measured in 10 mmol/L K^+ using dual-3′-FAM- and 5′-TAMRA-labeled c-*MYC* Pu22 DNA. (C) Top1 inhibitory activity at 50 μmol/L. (D) Top1 inhibitory activity of compounds **15g**, **13k**, **13h**, **13i**, **15h**, **15i** and **13e** ranging from 25 μmol/L to 12.5 μmol/L. (E) Top1 inhibitory activity of compounds **15g** and **15i** ranging from 10 μmol/L to 1 μmol/L. (F) Top2 inhibitory activity at 50 μmol/L.

ine the binding interactions of compound **15g** with c-*MYC*. Upon the addition of compound **15g**, obvious changes of the tetrad-guanine imino proton signals were observed, confirming the binding interactions (Fig. 3C). Western blotting and quantitative reverse transcription-polymerase chain reaction (qRT-PCR) assays were further performed using MCF-7 breast cancer cell line. MCF-7 cells were treated with compound **15g** at six concentrations (0, 1, 2.5, 5, 10 and 15 μmol/L) for 24 h. As shown in Figs. 3D and E, compound **15g** significantly reduced the levels of c-*MYC* protein and mRNA at the concentration of 2.5 μmol/L and 1 μmol/L, respectively. In contrast, rutaecarpine itself had no effect on the mRNA level and slightly decreased the c-*MYC* protein level at a high concentration of 10 μmol/L (Figs. 3D and E). These results further demonstrated the c-*MYC*G4 binding and stabilizing activity and c-*MYC* downregulation effect of compound **15g**.

To investigate the binding modes of compound **15g** with Top1 (PDB ID: 1T8I) [35], Top2α (PDB ID: 5GWK) [36] and c-*MYC*G4 (PDB ID: 2L7V) [37], molecular docking study was performed. As depicted in Fig. 4A, the lactam carbonyl group in the backbone of compound **15g** formed a hydrogen bond with Met428 of Top1. Electrostatic interactions between the amino-containing side chain and DNA base DT10 and TGP11 were observed. As for Top2α, Ser763 was interacted with the scaffold of compound **15g** through a hydrogen bond, and the side chain formed another hydrogen bond with Arg487 (Fig. 4B). As shown in Fig. 4C, compound **15g** could strongly stabilize c-*MYC*G4 with two of compound **15g** binding to the 5′- and 3′-terminal sites of the c-*MYC*G4. Specifically, the indole and benzopyrimidine moiety in the skeleton of compound **15g** in the 3′-site formed π-π stacking interactions with DG13 and DG18, respectively. In addition, the NH in the side chain formed a hydrogen bond with DT23. Similarly, the scaffold of compound **15g** formed π-π stacking interactions with the 5′-external tetrads, including DG7, DG11 and DG16. Additionally, a hydrogen bond between the side chain and DG5 was observed.

Using a competition fluorescence displacement assay [19], we further determined the binding selectivity of compound **15g** for c-*MYC*G4 as compared to a parallel K-Ras promoter G4, a hybrid telomeric G4, and double-stranded (ds) DNA (Fig. 5A). The competition fluorescence displacement assay allows for a straightforward assessment of selective binding toward c-*MYC*G4 *vs* the competitors, namely c-*MYC*G4s (parallel), telomeric G4 (hybrid), ds-DNA and K-Ras G4 (parallel). As shown in Fig. 5A, compound **15g** showed preferable binding selectivity for parallel and hybrid G4s (c-*MYC*G4, K-Ras G4 and telomeric G4) over dsDNA, and showed much more selectivity against c-*MYC*G4s. This result suggested that compound **15g** is a selective c-*MYC*G4 ligand to some degree but its c-*MYC*G4 selectivity still need to be improved.

The *in vitro* antitumor activity of compound **15g** against four human cancer cell lines (MCF-7 breast cancer cells, MDA-MB-231 breast cancer cells, HCT116 colon cancer cells and HeLa cervical cancer cells) were tested using the CCK8 assay. Camptothecin (CPT) was used as the positive control (Table S1). Compound **15g** showed potent antitumor activity with an IC_{50} value in the range of 1.7-3.3 μmol/L (Fig. 5B). The aqueous solubility was further evaluated under physiological conditions. Compound **15g** exhibited moderate aqueous solubility with 41.6 μg/mL at pH 7.4.

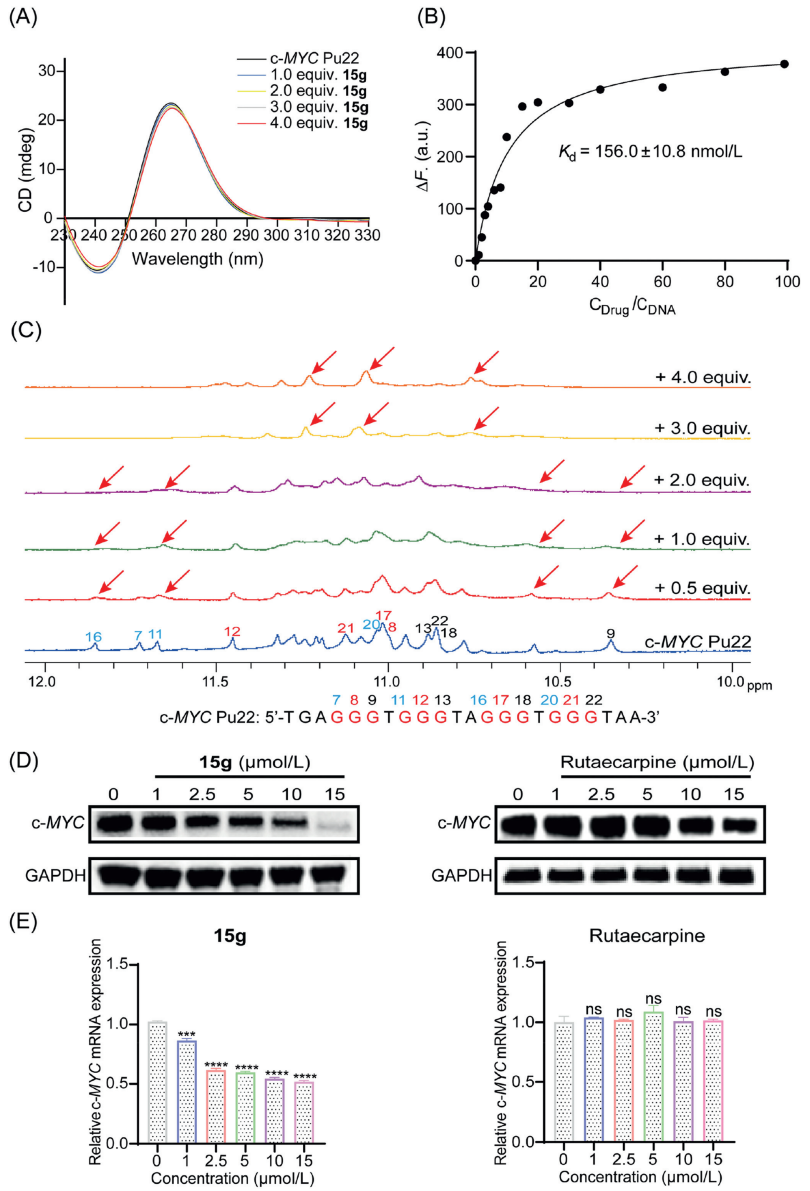

Fig. 3. c-*MYC* inhibitory activities of compound **15g**. (A) The signature of c-*MYC*G4 in the presence of compound **15g** by the CD titration assay. (B) Binding affinity of compound **15g** with c-*MYC*G4 using fluorescence-based binding assay. (C) Imino proton regions of the 1D ^{1}H NMR spectra of c-*MYC* Pu22 either alone or with compound **15g**. (D) Effects of compound **15g** and rutaecarpine on the transcription of c-*MYC* oncogene in MCF-7 cells by Western blotting. (E) Effects of compound **15g** and rutaecarpine on the c-*MYC* expression in MCF-7 cells by RT-PCR. ns = not significant, $^{***}P < 0.001$, $^{****}P < 0.0001$ *vs.* control group, determined with Student's *t*-test. At least two independent experiments were done for each condition.

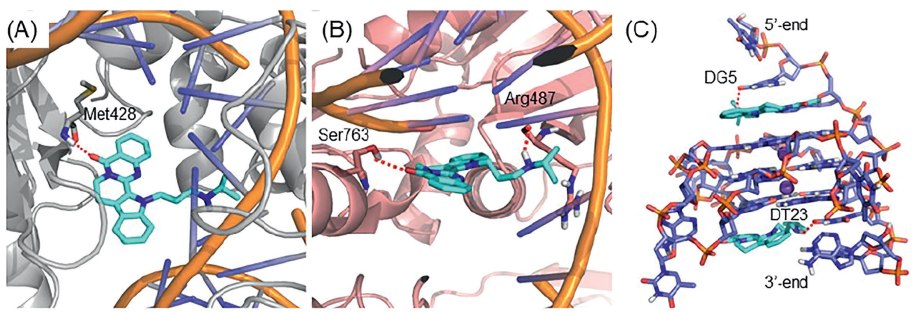

Fig. 4. The binding modes of compound **15g**. Proposed molecular interaction models of compound **15g** with Top1 (A), Top2 (B) and c-*MYC*G4 (C).

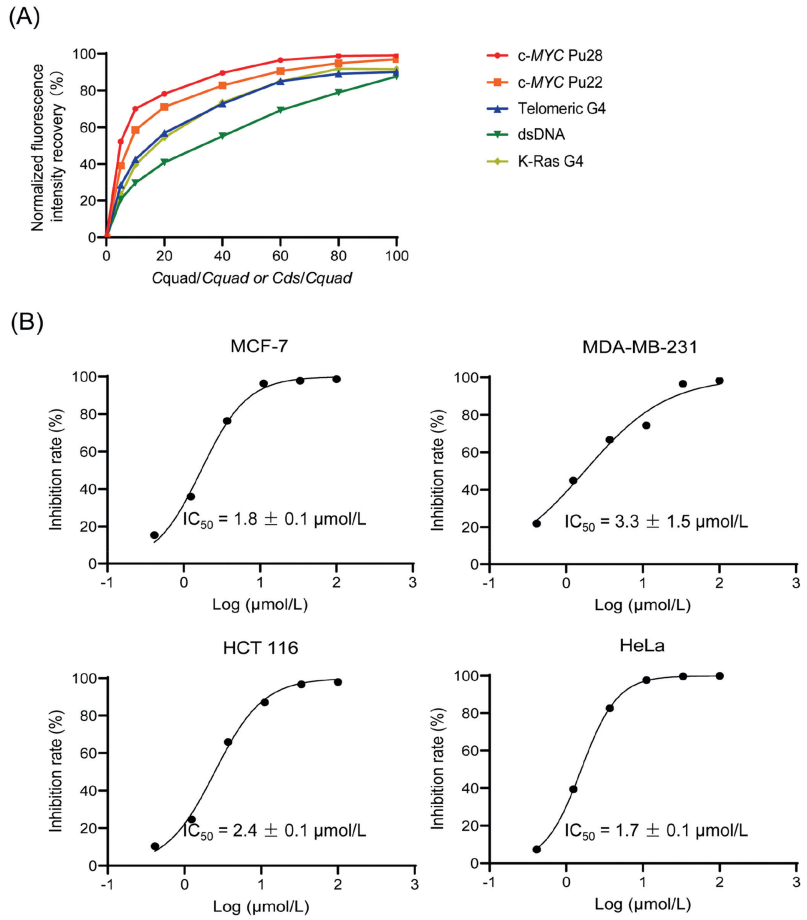

Fig. 5. G4 binding selectivity (A) and *in vitro* antitumor potency (B) of compound **15g**. At least two independent experiments were done for each condition.

Moreover, the effects of compound **15g** on the induction of apoptosis and cell-cycle in MCF-7 cells were evaluated by flow cytometry. As shown in Fig. S3A (Supporting information), compound **15g** induced the apoptosis of MCF-7 cells in a concentration-dependent manner. After the exposure of compound **15g** to various concentrations (1, 5 and 15 μmol/L) for 24 h, the percentages of apoptotic cells were 25.48%, 32.82%, and 73.01%, respectively. These results demonstrated that compound **15g** could effectively inhibit cancer cell growth through apoptosis induction. After the treatment with 1, 5, and 15 μmol/L compound **15g** for 24 h, the percentage of cells in the G2 fraction increased from 21.97% to 61.41% with a concomitant decrease in the proportion of cells in other phases of the cell cycle, suggesting the G2 cell-cycle arrest in MCF-7 cells (Fig. S3B in Supporting information).

In summary, this work reported novel triple G4 and Top1/2 ligands inspired by the indolopyridoquinazoline scaffold of natural products evodiamine and rutaecarpine. A focused library of 55 indolopyridoquinazoline analogues were rationally designed and synthesized. Notably, compound **15g** was proven to be a potent antitumor lead compound by triple targeting c-*MYC*G4 and Top1/2. Among the reported rutaecarpine derivatives, compound **15g** represents a highly potent compound in terms of *in vitro* antitumor activity. It may be used a valuable chemical tool to investigate the biological functions of c-*MYC*G4 and Top1/2. This proof-of-concept study validated the feasibility of using the planar scaffolds of natural products as templates to design new c-*MYC*G4 ligands. However, the antitumor potency and c-*MYC* G-quadruplex selectivity of compound **15g** still need to be further improved. Taken together, compound **15g** is a lead compound for the discovery of novel antitumor agents and further structural optimizations are in progress.

Declaration of competing interest

The authors declare that they have no known competing financial interests or personal relationships that could have appeared to influence the work reported in this paper.

Acknowledgments

This work was supported by the National Natural Science Foundation of China (Nos. 22077138 to S. Wu, 81725020 to C. Sheng, and 81872742 to G. Dong), the National Key Research and Development Program of China (No. 2020YFA0509200 to C. Sheng) and Shanghai Rising-Star Program (No. 22QA1411300 to S. Wu).

Supplementary materials

Supplementary material associated with this article can be found, in the online version, at doi:10.1016/j.cclet.2022.07.014.

References

[1] Y. Pommier, Y. Sung, S.N. Huang, J.L. Nitiss, Nat. Rev. Mol. Cell Biol. 17 (2016) 703–721.
[2] J.L. Delgado, C.M. Hsieh, N.L. Chan, H. Hiasa, Biochem. J. 475 (2018) 373–398.
[3] A. Thomas, Y. Pommier, Clin. Cancer Res. 25 (2019) 6581–6589.
[4] A. Ali, S. Bhattacharya, Bioorg. Med. Chem. 22 (2014) 4506–4521.
[5] B. Li, C.M. Gao, Q.S. Sun, et al., Chin. Chem. Lett. 25 (2014) 1021–1024.
[6] M.J. Piccart-Gebhart, N. Engl. J. Med. 354 (2006) 2177–2179.
[7] T.M. Ou, Y.J. Lu, C. Zhang, et al., J. Med. Chem. 50 (2007) 1465–1474.
[8] H.J. Kang, H.J. Park, Biochem 48 (2009) 7392–7398.
[9] A. Siddiqui-Jain, C.L. Grand, D.J. Bearss, L.H. Hurley, Proc. Natl. Acad. Sci. U. S. A. 99 (2002) 11593–11598.
[10] H.L. Cai, C.S. Zhou, Q.F. Yang, et al., Chin. Chem. Lett. 29 (2018) 531–534.

[11] Z. Yu, W.B. Huang, L.Q. Shi, S.Y. Ke, S.Z. Xu, Chin. Chem. Lett. 33 (2022) 1627–1631.
[12] G.W. Collie, G.N. Parkinson, Chem. Soc. Rev. 40 (2011) 5867–5892.
[13] C. Platella, C. Riccardi, D. Montesarchio, G.N. Roviello, D. Musumeci, Biochim. Biophys. Acta: Gen. Subj. 1861 (2017) 1429–1447.
[14] W.Q. Liu, Y.L. Xu, X. Li, et al., Chin. Chem. Lett. 32 (2021) 2322–2326.
[15] S. Balasubramanian, S. Neidle, Curr. Opin. Chem. Biol. 13 (2009) 345–353.
[16] G. Biffi, D. Tannahill, J. Miller, W.J. Howat, S. Balasubramanian, PLoS One 9 (2014) e102711.
[17] C. Platella, E. Napolitano, C. Riccardi, D. Musumeci, D. Montesarchio, J. Med. Chem. 64 (2021) 3578–3603.
[18] M.H. Hu, J.H. Lin, J. Med. Chem. 64 (2021) 6720–6729.
[19] K.B. Wang, M.S.A. Elsayed, G.H. Wu, et al., J. Am. Chem. Soc. 141 (2019) 11059–11070.
[20] F. Palluotto, A. Sosic, O. Pinato, et al., Eur. J. Med. Chem. 123 (2016) 704–717.
[21] M. Read, R.J. Harrison, B. Romagnoli, et al., Proc. Natl. Acad. Sci. U. S. A. 98 (2001) 4844–4849.
[22] A.M. Burger, F.P. Dai, C.M. Schultes, et al., Cancer Res. 65 (2005) 1489–1496.
[23] C. Martins, M. Gunaratnam, J. Stuart, et al., Bioorg. Med. Chem. Lett. 17 (2007) 2293–2298.
[24] H. Xu, M. Di-Antonio, S. McKinney, et al., Nat. Commun. 8 (2017) 14432.
[25] T.M. Ou, J. Lin, Y.J. Lu, et al., J. Med. Chem. 54 (2011) 5671–5679.
[26] R. Chaudhuri, S. Bhattacharya, J. Dash, S. Bhattacharya, J. Med. Chem. 64 (2020) 42–70.
[27] H. Yu, H. Jin, W.Z. Gong, Z.L. Wang, H.P. Liang, Molecules 18 (2013) 1826–1843.
[28] K.M. Tian, J.J. Li, S.W. Xu, Pharmacol. Res. 141 (2019) 541–550.
[29] S.I. Kim, S.H. Lee, E.S. Lee, C.S. Lee, Y.D. Jahng, Arch. Pharm. Res. 35 (2012) 785–789.
[30] G.Q. Dong, C.Q. Sheng, S.Z. Wang, et al., J. Med. Chem. 53 (2010) 7521–7531.
[31] G.Q. Dong, S.Z. Wang, Z.Y. Miao, et al., J. Med. Chem. 55 (2012) 7593–7613.
[32] S.Z. Wang, K. Fang, G.Q. Dong, et al., J. Med. Chem. 58 (2015) 6678–6696.
[33] F. Kouzine, S. Sanford, Z. Elisha-Feil, D. Levens, Nat. Struct. Mol. Biol. 15 (2008) 146–154.
[34] F. Kouzine, D. Levens, Front. Biosci. 12 (2007) 4409–4423.
[35] B.L. Staker, M.D. Feese, M. Cushman, et al., J. Med. Chem. 48 (2005) 2336–2345.
[36] Y.R. Wang, S.F. Chen, C.C. Wu, et al., Nucleic Acid. Res. 45 (2017) 10861–10871.
[37] J.X. Dai, M. Carver, L.H. Hurley, D.Z. Yang, J. Am. Chem. Soc. 133 (2011) 17673–17680.